# Analyst

Accepted Manuscript


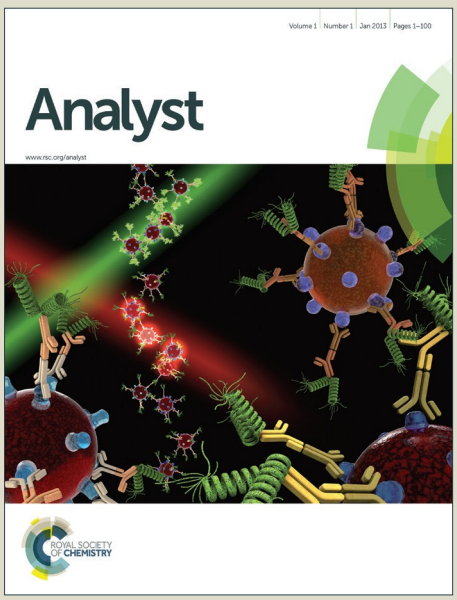





ROYAL SOCIETY OF CHEMISTRY

www.rsc.org/analyst

Journal Name

RSCPublishing

ARTICLE

# Magnetic high throughput screening system for the development of nano-sized molecularly imprinted polymers for controlled delivery of curcumin

**Elena V. Piletska,* Bashar Abd Hatem, Agata S. Krakowiak, Anitha Parmar, Demi L. Pink, Katie S. Wall, Luke Wharton, Ewa Moczko, Michael J. Whitcombe, Kal Karim, Sergey A. Piletsky**

**Cite this: DOI: 10.1039/x0xx00000x**

Received 00th January 2012,
Accepted 00th January 2012

DOI: 10.1039/x0xx00000x

**www.rsc.org/**

Curcumin is a versatile anti-inflammatory and anti-cancer agent known for its low bioavailability, which could be improved by developing materials capable of binding and releasing drug in a controlled fashion. The present study describes the preparation of magnetic nano-sized Molecularly Imprinted Polymers (nanoMIPs) for the controlled delivery of curcumin and their high throughput characterisation using microtitre plates modified with magnetic inserts. NanoMIPs were synthesised using functional monomers chosen with the aid of molecular modelling. The rate of release of curcumin from five polymers was studied under aqueous conditions and was found to correlate well with the binding energies obtained computationally. The presence of specific monomers was shown to be significant in ensuring effective binding of curcumin and to the rate of release obtained. Characterisation of the polymer particles was carried out using dynamic light scattering (DLS) technique and scanning electron microscopy (SEM) in order to establish the relationship between irradiation time and particle size. The protocols optimised during this study could be used as a blueprint for the development of nanoMIPs capable of the controlled release of potentially any compound of interest.

## Introduction

Curcumin is an orange-yellow, plant-based polyphenol derived from turmeric. The commercial form of this compound, curcuminoid, is available as a colouring agent or food additive which is comprised of 77% curcumin, 18% demethoxycurcumin and 5% bisdemethoxycurcumin,[1] with a recommended daily dosage of 0-3 mg (kg day)$^{-1}$ when used as a spice.[2] Turmeric and other curcumin containing compounds have traditionally been used in ancient Chinese and Indian medicine due to their antiseptic, anti-inflammatory and antioxidant properties. The anti-inflammatory effect of curcumin has been utilised in the treatment of diseases ranging from oedema to pancreatitis.[3] Studies carried out on rats showed that curcumin could be used as an effective symptomatic treatment for rheumatoid arthritis, whilst rats with pancreatitis displayed significant decrease in anti-inflammatory markers.[4]

Department of Chemistry, College of Science and Engineering, University of Leicester, LE1 7RH, UK; *Corresponding author: Email: ep219@le.ac.uk; Tel: +44(0)116 294 4669.

Therefore, it is likely that the medicinal properties of curcumin can be useful for future human applications. Notably, South-East Asia presents a distinctly lower occurrence of specific cancers in comparison to western countries, with the rate of colon cancer in men at 4.7 per 100,000 population in India, contrasting the 40.6 per 100,000 diagnosed in the United States.[5] These stark differences are mirrored in lung and breast cancer statistics and can be correlated, partially, to the comparative dietary intakes of turmeric. Current research has suggested turmeric can act as a growth inhibitor for strains of *Heliobacter pylori*, which in high concentrations has been linked to increased risk of stomach and colon cancer, with ingestion of turmeric proving to lower the chance of these cancers. This evidence suggests curcumin's potential usefulness in both preventative and therapeutic anti-cancer treatments.[6]

A study investigating the effect of curcumin on several types of cancer revealed that polyphenol arrested growth of numerous tumour cells including melanoma, colon and breast carcinoma. The inhibition of tumour cell growth by curcumin ultimately results in apoptosis of the targeted cells, with the pathway curcumin acts upon to induce apoptosis being specific

to the tumour type. Potential routes include activation of the tumour suppressor p53 pathway, which can signal cell death by altering cellular redox states.[7]

Significantly, curcumin based cancer therapeutics have reached clinical trials, with a phase 1 study on 15 advanced colorectal cancer patients on a 3.6 g dosage showing a decrease of up to 46% in PGE2 levels. This prostaglandin is a product of COX-2, which stimulates growth of cancer cells within the colon. This indicates that the reduction of tumour growth in patients was a result of curcumin administration.[8] Further trials on colorectal cancer patients saw a higher (8 g) dose of curcumin tolerated for at least 18 months with no adverse side effects. A distinct correlation between larger dosages and longer stabilisation periods was presented through these studies[9], with only minimal toxicity being noted at doses of 12 g.[10]

The biological activity of curcumin provides a valuable foundation for future drug development and therapeutics. The progression of novel drug delivery systems could be effective in maximising the potential of this compound in the body, thus overcoming its low bioavailability.[10] Nanoparticle technology of phytochemicals remains a frontier in medical research, with nanoformulations of curcumin improving efficacy, tumour targeting and reducing the systemic toxicity of the compound.[11]

Despite significant therapeutic value, curcumin's low bioavailability results in only small portions of the administered dose entering the bloodstream due to the rapid rate at which the compound is metabolised. Studies demonstrated that 3.6 g of curcumin taken orally gave detectable plasma levels of curcumin after 1 hr, whilst doses of 2 g were untraceable in the bloodstream. Therefore >3.6 g of curcumin is considered an effective starting dose against multiple illnesses. It is very important to develop curcumin-specific materials, which are capable of binding to and releasing the drug in order to provide its controlled delivery and reduce the necessity to use repeated high doses in potentially toxic quantities.[12]

Furthermore, with the majority of nanoformulations presenting a standard biphasic pattern of release in vitro, this paper studies the novel use of MIPs for a more controlled release of curcumin.[11] By investigating the specific binding strength of different biocompatible monomers to the template molecule, and subsequent effect on curcumin release over time, it can be determined which nanoMIPs may be suitable for future biological applications in drug delivery systems. With the amount of drug release directly correlating to the concentration of active curcumin at the target site, thus extent of therapeutic effect, this study may highlight the potential of MIPs in sustained and targeted drug release.

Current strategies for nanoencapsulation of curcumin range from SNLs to PLGA, achieving a two-fold increase in bioavailabilty, with the polymeric nanoformulations demonstrating better drug-loading ability compared to non-polymer formulations with uptake of up to 97.5% in PLGA.[11, 13]

A wide variety of methods could be employed for the quantification of curcumin. Such techniques include UV-visible and fluorescence spectroscopy, high performance thin layer chromatography (HPTLC), nuclear magnetic resonance (NMR) spectrometry and mass spectroscopy (MS).[14] It is known that curcumin absorption wavelength and molar absorptivity values depend on the environment, especially solvents. Detection limits using UV-visible spectroscopy are 0.1-15 ppm and with fluorescence spectroscopy is 0.34 ppb.[14] Due to the ability of curcumin to absorb light in the visible spectrum we demonstrated here how a generic multititre plate reader could be used for screening of the magnetic nanoMIPs allowing their selection and development to be facilitated.

## Materials and Methods

### Materials

Curcumin, trimethylopropane trimethacrylate (TRIM), ethylene glycol methacrylate phosphate (EGMP), 2-hydroxyethyl methacrylate (HEM), tetraethylthiuram disulphide, methacrylic acid (MAA), itaconic acid (ITA), iron (II, III) oxide and sodium diethyldithiocarbamate trihydrate were purchased from Sigma-Aldrich (Gillingham, UK). Sodium monohydrogen phosphate dibasic, sodium dihydrogen phosphate monobasic and diethylamine were purchased from ACROS Organics (Loughborough, UK). Acetonitrile (HPLC grade) was purchased from VWR Probolabo Chemicals (Lutterworth, UK). Chloroform was purchased from Fisher Scientific (Loughborough, UK). Benzyl chloride was purchased from Lancaster Synthesis (Newgate, UK). Diethyldithiocarbamic acid benzyl ester was synthesised in house.

### Diethyldithiocarbamic acid benzyl ester

This compound was synthesised according to the method of Henckens *et al.*[15] To a stirred solution of benzyl chloride (10.0 g) in ethanol (50 mL) was added sodium diethyldithiocarbamate trihydrate (19.6 g). The suspension was stirred at room temperature for 2 h. Water (200 mL) was added and the product extracted with CHCl3 (3 × 50 mL). The combined organic extracts were washed with water (2 × 50 mL), dried ($MgSO_4$) and evaporated to yield the title compound as a light yellow oil (13.7 g, 72%). $^1$H NMR (CDCl3): 1.31 (2 × t, 6H), 3.76 (q, 2H), 4.08 (q, 2H), 4.58 (s, 2H), 7.18-7.33 (5H). 13C NMR ($CDCl_3$): 11.63, 12.51, 42.24, 46.74, 49.49, 127.46, 128.58, 129.41, 136.06, 195.28.

### Molecular modelling

Monomer-template interactions were simulating using the SYBYL 7.3 (Tripos Inc. ST. Louis, MO, USA) software package in conjunction with the SPECTRE operating system at the University of Leicester. Multiple optimised structures of curcumin were generated by minimisation of charged templates to a value of 0.001 kcal $mol^{-1}$ and two conformations with the lowest energies were selected for further interpretation. Simulated dynamics were carried out over a 700 - 300 K temperature range for 100,000 iterations at each temperature, to ensure that the most energetically favourable structures were obtained. A database consisting of 28 monomers was screened



 

against the subsequent structures using a Leapfrog algorithm performed for 60,000 iterations, to determine the interactions between the template and monomers.[16, 17] The Leapfrog results provided binding energies for the monomers tested and those with high, medium and low affinity (ITA, EGMP, MAA and HEM) were selected for further investigation.

**Optimisation of irradiation time**

Polymer containing MAA functional monomer was selected for the optimisation of the polymerisation time. A series of ten vials was prepared to monitor the rate of polymer formation upon irradiation with UV light, each containing 10 mg of iron (I, III) oxide nanoparticles. In a separate container 0.1 mmol of curcumin and 1 mmol of MAA were added to 5 g of acetonitrile. This was mixed with cross-linker TRIM (4.6 g), chain terminator tetraethylthiuram disulphide (50 mg) and iniferter diethyldithiocarbamic acid benzyl ester (2.5 mg). Equal amounts of the monomeric mixture were then added to the vials containing 10 mg of the paramagnetic iron oxide particles.

The solutions were irradiated under a Philips UV lamp for 120 minutes and then one of the vials was subsequently removed every 20 minutes thereafter. The polymer-modified magnetic particles were collected using a magnet whilst the remaining solution was discarded. The vials were then weighed and the differences in mass recorded.

**Preparation of the polymers**

Based on results obtained from molecular modelling, four monomers with varying affinities towards curcumin were chosen- EGMP, ITA, MAA and HEM. A standard 1:4 molar ratio of curcumin to monomer was used to attain a solution containing 0.1 mmol of curcumin and 0.4 mmol of monomer.

A monomeric solution composed of acetonitrile (30 g), TRIM (29.1 g), iniferter - diethyldithiocarbamic acid benzyl ester (15 mg), chain terminator agent - thiuram disulphide (300 mg) and curcumin (222 mg) was prepared. 10 mL of the monomeric solution was added to each vial containing 0.4 mmol of each monomer (Table 1).

**Table 1:** Composition of the polymers.

| Polymer name | Template, mg | Func. mon., mg | Cross-linker (TRIM), g | Solvent, g | Inif., mg | Chain termin., mg |
|---|---|---|---|---|---|---|
| HEM | 37 | 52.5 | 4.9 | 5 | 2.5 | 50 |
| MAA | 37 | 37.0 | 4.9 | 5 | 2.5 | 50 |
| ITA | 37 | 52.5 | 4.9 | 5 | 2.5 | 50 |
| EGMP | 37 | 86.2 | 4.9 | 5 | 2.5 | 50 |
| Control | 37 | 0 | 4.9 | 5 | 2.5 | 50 |

The vials were then irradiated under a UV lamp (Philips, UK) for 150 minutes. After the polymerisation the vials were wrapped in aluminium foil and kept in the fridge. A control polymer without any functional monomer was also produced, using the procedure outlined above. The obtained magnetic nanoMIPs were collected using a magnet, washed twice with acetonitrile (2 x 15 mL) and stored in the fridge in distilled water (15 mL). The mass of all obtained magnetic nanoMIPs was calculated by subtraction of the initial weight of the vials from the weight of the magnetic nanoMIPs measured after polymerisation and also after washing with acetonitrile. In order to ensure the complete removal of un-reacted monomers washing with acetonitrile (5 × 10 mL) was applied. All handling (weighing and exchange of the liquid or washing) of the magnetic particles was done using a magnet. The polymer-containing magnetic particles were collected using the magnet for one hour. The liquid was removed and pellet was dried at a room temperature for 30 min before the weighing.

Non-imprinted Polymers (NIPs) were produced using the same synthetic procedure outlined for the MIPs in the absence of curcumin in the reaction mixture.

**Physical characterisation of the magnetic nanoparticles**

The size of all produced magnetic nanomaterials was characterised using Nano-S Zetasizer Particle Size Analyser (Malvern Instruments, UK) by executing a dynamic light scattering (DLS) technique. Before the measurement all polymeric fractions were ultrasonicated for 3-5 min and diluted to 10 mg $mL^{-1}$ with water. DLS measurements of the samples without filtration and sonication pre-treatment were also made in order to assess the properties of the obtained particles.

A scanning electron microscopy (SEM) was used for the characterisation of magnetic nanoparticles. Nanoparticles samples were analysed using FEI XL30 Environmental Scanning Electron Microscope (Philips, UK). Analysis was performed using an accelerating voltage of 20 kV.

**Study of curcumin release from magnetic nanomaterials**

Magnetic polymer particles were synthesised as outlined above using HEM, MAA, EGMP and ITA as functional monomers. Control polymers were also synthesised under the same conditions, with no functional monomer present in the reaction mixture.

Microtitre plates modified with magnetic inserts were prepared as described by Piletska.[18] The magnetic inserts were attached to each of the sample wells to allow efficient immobilisation of the magnetic particles.

In order to rebind the curcumin, samples of each of the magnetic particle preparations (20 mg) were weighed and incubated with a solution of curcumin in acetonitrile (1.5 mL, 1 mg $mL^{-1}$) for 12 h. After the incubation the magnetic particles were collected using the magnet and curcumin solution in acetonitrile was removed. Then, the magnetic nanoparticles were re-suspended in 25 mM phosphate buffer, pH 7.0 (1 mL) and 100 μL-aliquots were added to the wells of the microtitre plate equipped with magnetic inserts. Typically, 6 replicates of each sample were tested. A waiting time of 5 min was given to allow the magnetic polymers to be immobilised on the magnetic inserts and clear optical path through the well, the optical density of the solution was recorded at a wavelength of 405 nm at 10 minute intervals using a microtitre plate reader (Dynex, UK). Due to curcumin's low stability in aqueous solution, the microtitre plate was protected from the light between measurements by covering with aluminium foil.

### Quantification of curcumin release in batch experiments

Magnetic particles (100 mg) were collected from each of the respective stock solutions and a solution of curcumin in acetonitrile (1.5 mL, 1 mg $mL^{-1}$) was added. The samples were allowed to equilibrate and re-bind the template during a period of 12 hours (overnight). Efficient separation of the polymer particles was achieved using a magnet, enabling an analysis of the particles-free solution using a UV-vis spectrophotometer. A wavelength of 415 nm was selected as the most appropriate[14] to monitor the difference in curcumin adsorbed between MIP and corresponding NIP particles. The magnetic nanoMIPs and nanoNIPs particles were transferred into aliquots of 25 mM phosphate buffer pH 7.0 (5 mL). The release of curcumin from the nanoparticles after incubation in the buffer solution was measured using a spectrophotometer. A standard procedure involving mixing and separation using a magnet was applied.

## Results and discussion

### Chemical properties of curcumin

Two phenolic OH-groups alongside the enolic proton (Fig. 1) give curcumin three distinct $pK_a$ values at 7.75-7.80, 8.55 and 9.05.[2]

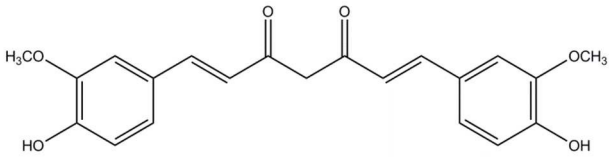


**Fig. 1** Molecular structure of curcumin.

The molecule of curcumin is soluble in both, polar and nonpolar solvents. It was observed that in aqueous solutions curcumin is more stable under acidic than at basic conditions, which is also reflected in its higher absorbance coefficient. Similarly, temperature also shows implications for the stability of curcumin: decomposition setting in when heated to 70 °C and above. When in solution curcumin is also sensitive to light. Due to its limited stability the development of materials capable of binding to and controlled release of curcumin would allow the administration of effective quantities of the drug without the need to expose the organism to deliberately excessive doses.

### Molecular modelling

A molecular model of curcumin was produced using Sybyl 7.3 operating software. Computational procedures were carried out to obtain the lowest energy conformations; the template was drawn and charged, minimised to 0.001 kcal $mol^{-1}$ over 30,000 iterations and simulated dynamics performed, followed by further minimisation. The resulting structures (Fig. 2) were screened against a monomer database using the Leapfrog algorithm, and each functional monomer ranked according to its binding score.

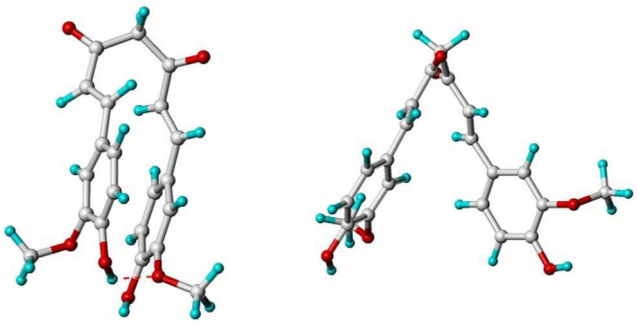

**Structure 1** **Structure 2**

**Fig. 2** Lowest energy's structures of curcumin (Structure 1: -8.171 kcal $mol^{-1}$, Structure 2: -10.595 kcal $mol^{-1}$).

**Table 2:** Neutral (N) and charged (-) monomers with corresponding binding affinities for curcumin.

| Structure 1 | | Structure 2 | |
|---|---|---|---|
| **Monomers** | **Binding energy, kcal $mol^{-1}$** | **Monomers** | **Binding energy, kcal $mol^{-1}$** |
| EGMP (-) | -43.23 | EGMP (-) | -31.71 |
| ITA (N) | -37.22 | ITA (N) | -30.89 |
| ITA (-) | -34.58 | EGMP (N) | -30.22 |
| EGMP (N) | -33.86 | ITA (-) | -29.93 |
| HEM (N) | -30.01 | MAA (-) | -28.15 |
| MAA (N) | -23.83 | MAA (N) | -24.81 |
| MAA (-) | -22.32 | HEM (N) | -23.48 |

Negatively charged EGMP was found to have the highest affinity for the template, with binding scores of -43.23 kcal $mol^{-1}$and -31.71 kcal $mol^{-1}$ in each configuration, respectively. The strength of molecular complexes formed between curcumin and EGMP is reflected by the strength of the hydrogen bonding interactions between the functional groups in each constituent. Accordingly to the molecular modelling the phosphate functional group in EGMP interacts strongly with the hydroxyl groups in curcumin resulting in the stabilised molecular complexes obtained (Fig. 3). The lower binding scores for the remaining monomers are also a consequence of the strength of hydrogen bonding interactions with the template functional groups. For instance, the Leapfrog algorithm determined the interactions of MAA with the template to be weaker than EGMP due to the strength and number of hydrogen bonds in the molecular complex. The molecular complex formed using the monomer MAA shows a single-point interaction between the carboxylic group and a hydroxyl of the template, which reflects the lower calculated binding score (Fig. 3).

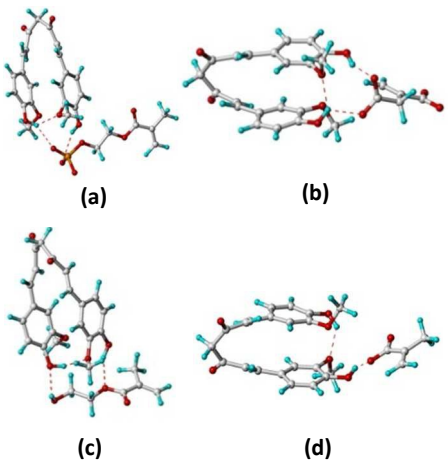


**Fig 3** Interactions between curcumin (Structure 1) and monomers (a) EGMP, (b) ITA, (c) HEMA and (d) MAA.

Further analysis allowed monomer-template ratios suitable for synthetic testing to be obtained. Solvation of the template with each monomer, and subsequent minimisation to 0.005 kcal $mol^{-1}$ over 200,000 iterations, gave realistic models of the behaviour of monomers with curcumin in solution. Interpretation of intermolecular and intramolecular interactions in each model, shown in Fig. 3, could be used to further optimise the synthesis conditions. The application of monomer-template ratios from the simulated annealing to the synthetic procedure should result in more highly selective MIPs with sufficiently enhanced controlled release.

### Optimisation of polymer preparation

The protocol for the preparation of the nanoparticles was based on the method which was described by Subrahmaniam.[19] In order to produce nanoparticles possessing magnetic properties iron oxide nanoparticles were added to the polymerisation mixture. In order to model real polymerisation conditions a monomeric mixture containing all necessary components, e.g. template (curcumin), cross-linker, iron oxide, iniferter, chain terminating agent, was used for the optimisation of the time of illumination.

It was found that there was a clear relationship between irradiation time and differences in the mass of magnetic nanoparticles, suggesting that a layer of polymer was formed on the surface of the iron oxide particles. It was also observed that, although the mass of the magnetic fraction was further increased by a lengthening of the polymerisation time, a gelation of the monomeric mixture, which occurred in vials 7-10, indicated that the maximum size achievable is limited by the irradiation time. Gelation was identified by a sharp decrease in particle size after 250 minutes of illumination (Fig. 4, fractions 7-10), which correlated with observed aggregation and settlement of the polymerised material on the wall of the glass vial. It was shown that 120-160 minutes is sufficient time for the formation of polymeric layer on the surface of iron oxide nanoparticles (Table 3).

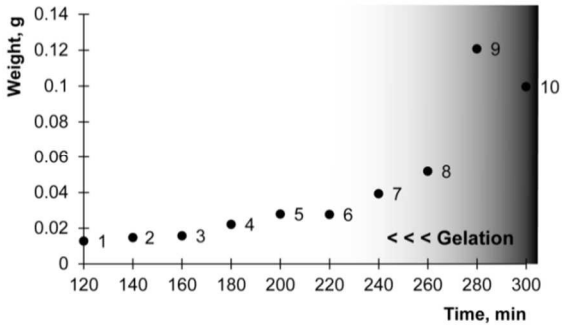


**Fig. 4** The dependence between the time of irradiation and mass of the polymer grafted onto the iron oxide particles (collected fractions are labelled by corresponding numbers).

**Table 3:** Correlation between the irradiation time and size of the polymeric fractions measured by DLS technique.

| Fraction | Time, min | Diameter, nm |
|---|---|---|
| Iron oxide | 0 | 256.5±27.6 |
| 1 | 120 | 738.8±141.7 |
| 2 | 140 | 886.2±100.9 |
| 3 | 160 | 885.6±54.7 |
| 4 | 180 | 1166.7±565.6 |
| 5 | 200 | 3085.7±555.9 |
| 6 | 220 | 713.7±94.5 |

Therefore, the irradiation time of 150 min was selected for the preparation of the magnetic nanoMIPs containing computationally-selected functional monomers.

Electron microscopy of the magnetic nanoparticles before and after polymerisation confirmed that the size of the particles had increased from 12-15 nm (iron oxide particles, Fig. 5a) to 25-30 nm (polymer-grafted iron oxide particles, Fig. 5b). It was found that the measurements of the size obtained using SEM technique were lower than that measured by DLS analysis, which could be explained by agglomeration of the particles in aqueous solution and also by the fact that SEM measures the size of the dry particles and DLS analyses the samples in solution and possibly in the swollen state.

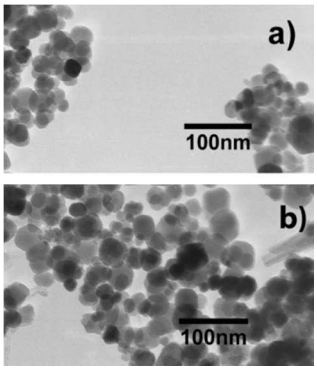


**Fig. 5** The SEM image of the iron oxide nanoparticles (a) and iron oxide grafted with polymer (b).

### Preparation and physical characterisation of the nanoMIPs containing selected functional monomers

A series of magnetic nanoMIPs and nanoNIPs were produced accordingly to the protocol described in the Materials and Methods section. The amount of polymer synthesised around the magnetic particles was calculated by subtraction of the weight of iron oxide particles used in the experiment from the total weight of the obtained magnetic nanoparticles after intensive washing with acetonitrile (Table 4). It was found that a similar quantity of the polymeric materials was produced (0.7-0.9 g per g of iron oxide particles) except in the case of the ITA-based polymer, which demonstrated a larger increase in weight (1.5- 3.9 g) (Table 4).

**Table 4:** Mass of the produced polymers per g of iron oxide particles.

| Monomer | MIP, g | NIP, g |
|---|---|---|
| Control | 0.94 | 0.78 |
| HEM | 0.96 | 0.8 |
| MAA | 0.85 | 0.84 |
| ITA | 1.47 | 3.9 |
| EGMP | 0.77 | 0.79 |

**High throughput testing of the curcumin release using microtitre plate equipped with magnetic inserts**

Monitored release of curcumin from the magnetic nanoMIPs using the modified microtitre plate was carried out over a 25-hour period, and results obtained for the initial release are shown in the Fig. 6.

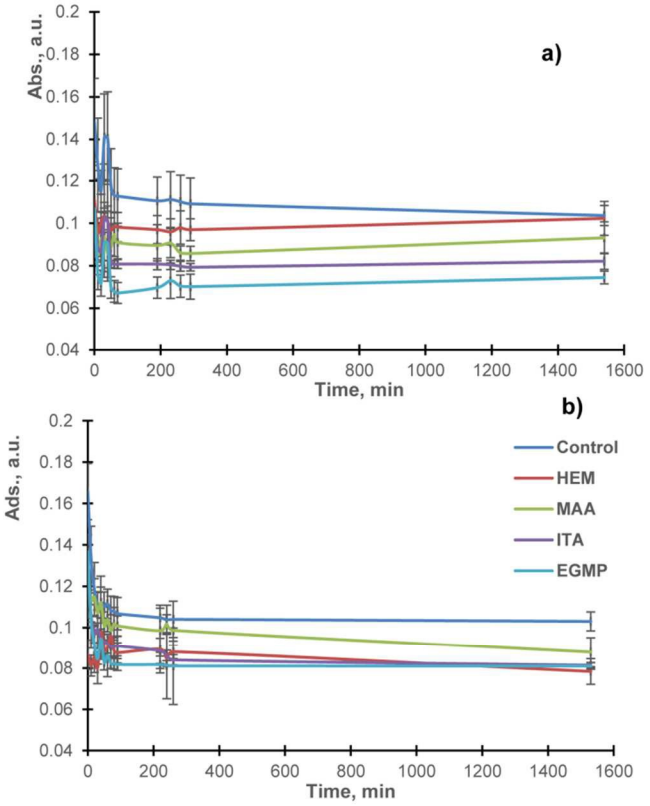


**Fig. 6** Curcumin release from corresponding imprinted and non-imprinted polymers in microtitre plates equipped with magnetic inserts.

The results obtained in the microtitre plate experiments indicate that the optimised synthetic procedure was successful in the production of molecularly imprinted polymers. The correlation between the level of curcumin release from the nanomaterials containing various functional monomers and their corresponding binding energies predicted using computational modelling was observed. It was expected that monomers with high affinity towards the template (e.g. EGMP and ITA) would produce more long-lived molecular complexes within the MIPs than those of weaker affinity (HEM or MAA). Hence, the rate of release of curcumin was directly related to strength of the monomer-template interactions; higher affinity monomers exhibited slower release rates, and vice versa. The fastest release rate was observed from the control polymers made without functional monomers, which suggest that the presence of functional monomers is very important for the development of the materials able to release the drugs with particular required rate.

Considerations about the charge of each of the functional monomer in the phosphate buffer (pH 7.0) have been made, and appropriate binding energies used to evaluate the results. It was expected that all polymers contained acidic functional monomers (EGMP, MAA and ITA), which were tested in the experiment, would be negatively charged at pH 7.0 used during the testing.[20]

It was observed that the nanoMIPs exhibited a delay in the release of curcumin, which is not observed with the NIPs, and provides further evidence for the presence of imprinted sites. The template exhibits a stronger affinity for the imprinted sites than towards the distributed randomly functional groups present at non-imprinted sites; hence the difference in the strength of interaction at these sites can account for the observed rates of release.

The EGMP-based nanoMIPs exhibited the strongest binding affinity towards the template and slowest controlled release of curcumin into the buffer solution, which was consistent with the results obtained using Leapfrog algorithm. The HEM-based polymer demonstrated the weakest affinity for the template, with rate of release being significantly greater than that of EGMP; thus, it is possible to conclude that the HEM-based polymer would be unsuitable for the application in controlled drug delivery. The control polymer which was prepared without any functional monomer demonstrated even faster release of the curcumin than the HEM-based polymer, which suggests that rational selection of the functional monomers is a very important factor for the preparation of the materials for the controlled drug delivery. It is also necessary to highlight that it is difficult to overestimate the benefit offered by computational modelling which was used to select suitable functional monomers and minimise time and resources required for the experimental research.

**Polymers characterisation**

The results of the DLS measurements confirmed that nanoparticles of similar sizes have been produced (Table 5) with the exception of ITA-based MIP nanoparticles, which had

larger size than other magnetic nanoparticles. This fact was in agreement with relatively high weight increase, which was observed after the grafting of ITA-based polymers in comparison with other polymers. Although ITA-based nanoparticles demonstrated high re-binding and a steady release of curcumin, however, due to the large particle size and tendency to aggregate, they could be unsuitable for biological or clinical applications.

The diameter of the particles in each sample was also measured without filtration, ultra-sonication or any other pre-treatment. It was found that all particles had size of roughly 1000 nm exhibiting quite high polydispersity, except EGMP-based nanoparticles, which were around 200 nm in diameter and had a low polydispersity index. This observation indicated EGMP had demonstrated lower tendency to aggregate in water, which may be due to the strong negative surface charge on the EGMP-based nanoparticles. It is possible to propose that further characterisation of the particles by zeta potential measurements could allow the stability of the particle solutions to be studied in greater detail. Small angle X-Ray scattering could also potentially be used to investigate agglomeration effects as well as to characterise the morphology and surface properties of the developed nanoparticles.

**Table 5:** Mean particle size of MIP and NIP-modified magnetic nanoparticles measured using DLS.

| Monomer | MIP, nm | NIP, nm |
|---|---|---|
| HEM | 242±16 | 142±13 |
| MAA | 198.66±25 | 265±24 |
| ITA | 811.12±35 | 187±17 |
| EGMP | 185.93±24 | 135±18 |
| Control | 237.84±13 | 249±26 |

**Characterisation of the magnetic nanopolymers using batch analysis**

In order to confirm the results of the microtitre plate screening of the library of polymers, the release of the curcumin was also investigated using a batch analysis. For this experiment larger quantity of the magnetic particles (100 mg) was incubated with 1 mg $mL^{-1}$ of curcumin in acetonitrile (2 mL) in order to re-bind the drug for the batch analysis experiment. The amount of curcumin adsorbed by all polymers was measured and quantified accordingly to a calibration curve, which was made using standard solutions of curcumin in acetonitrile. It was found that all produced MIP nanoparticles adsorbed more curcumin than corresponding NIPs, which confirms the finding that successful MIP grafting was achieved. Then it was placed in the glass vials containing 5 mL of 25 mM phosphate buffer, pH 7.0 and the optical absorbance of the solution was periodically measured. The magnetic properties of the tested polymers allowed collecting them easily using a magnet and analysing the particle-free supernatant. The optical density of the released curcumin was measured using a spectrophotometer and was quantified accordingly to the calibration curve prepared in 25 mM phosphate buffer, pH 7.0. It was observed that MIP-grafted nanoparticles have bound significantly more curcumin than NIP nanoparticles. MIP-grafted nanoparticles also provided slower release of curcumin in comparison with NIP-grafted magnetic particles, a fact that suggests that the molecular imprinting allowed the production of high affinity binding sites beneficiary for controlled delivery applications (Table 6).

**Table 6:**The results of the batch analysis of the MIP- and NIP-grafted nanoparticles.

| | Curcumin bound, μg $g^{-1}$ particles | | I | Curcumin release, μg $g^{-1}$ particles per day | | Predicted time of curcumin release, days | |
|---|---|---|---|---|---|---|---|
| | MIP | NIP | | MIP | NIP | MIP | NIP |
| Control | 291.0 | 219.0 | 1.3 | 112.9 | 238.6 | 2.6 | 0.9 |
| ITA | 417.0 | 277.0 | 1.5 | 101.2 | 376.9 | 4.1 | 0.7 |
| MAA | 444.0 | 240.0 | 1.9 | 139.3 | 186.1 | 3.2 | 1.3 |
| EGMP | 253.0 | 129.0 | 2.0 | 46.8 | 105.0 | 5.4 | 1.2 |

## Conclusions

A protocol for the preparation of magnetic nanoMIPs and their rapid screening was developed. It was shown that it is possible to prepare magnetic nanoMIPs exhibiting a steady release of curcumin with various rates, which suggests that such materials could be used as drug delivery systems. It was demonstrated that the magnetic properties of the synthesised particles in combination with microtitre plate equipped with magnetic inserts allows for the development of new bespoke drug delivery materials and for an optimisation of the polymer compositions quickly and effectively.

Potentially, the magnetic properties of the produced nanoMIPs could be used to target tumours that are very hard to access using traditional surgical methods by directing the particles inside the body using magnetic fields. It is foreseen that the application of specific magnetic drug delivery vehicles could potentially minimise the destructive influence of chemotherapy during cancer treatment. Of course, the development of magnetic polymeric particles presented here is just the first step towards clinical applications and some further biological testing will be required.

In conclusion, the proposed approach and optimised protocols are generic and could be used as a blueprint for the development of materials for the controlled release of any drug of interest.

**Acknowledgement** The authors would like to thank Stanislav Piletsky for manufacturing and supplying the magnetic disks for the microtitre plate experiment.

### Notes and references

1. P. Anand, C. Sundaram, S. Jhurani, A. B. Kunnumakkara and B. B. Aggarwal, *Cancer Lett*., 2008, **267**, 133.
2. M. Lestari and G. Indrayanto, *Profiles Drug Subst. Excip. Relat. Methodol.,* 2014, **39**, 113.
3 B. B. Aggarwal, C. Sundaram, N. Malani and H. Ichikawa, *Adv. Exp. Med. Biol.*, 2007, **595**, 1.
4. J. S. Jurenka, *Altern Med Rev*, 2009, **14**, 141.
5. J. Ferlay, H.-R. Shin, F. Bray, D. Forman, C. Mathers and D. M. Parkin, *Int. J. Cancer,* 2010, **127**, 2893.

6. R. De, P. Kundu, S. Swarnakar, T. Ramamurthy, A. Chowdhury, G. Balakrish Nair and A. K. Mukhopadhyay, *Antimicrob. Agents Chemother.,* 2009, **53**, 1592.
7. B. B. Aggarwal, A. Kumar and A. C. Bharti, *Anticancer Res.*, 2003, **23**, 363.
8. R. A. Sharma, H. R. McLelland, C. R. Ireson, K. A. Hill, S. A. Euden, M. M. Manson, M. Primohamde, L. J. Marnett, A. J. Gescher and W. P. Steward, *Clin. Cancer Res*., 2001, **7**, 1894.
9. R. A. Sharma, S. A. Euden and S. L. Platton, *Clin. Cancer Res*., 2004, **10**, 6847.
10. N. Dhillon, B. B. Aggarwal and R. A. Newman, *Clin. Cancer Res*., 2008, **14**, 4491.
11. M. Murali and S. Yallapu, *Curr. Pharm. Des*., 2013, **19**, 1994.
12. P. Anand, A. B. Kunnumakkara, R. Newman and B. B. Aggarwal, *Mol. Pharm*., 2007, **4**, 807.
13. S. Wang, R. Su, S. Nie, M. Sun, J. Zhang, D. Wu and N. Moustaid-Moussa, *J. Nutr. Biochem*., 2014, **25**, 363.
14. M. Lestari and G. Indrayanto, *Profiles Drug Subst. Excip. Relat. Methodol.,* 2014, **39**, 113.
15. A. Henckens, I. Duyssens, L. Lutsen, D. Vanderzande and T. J. Cleij *Polymer*, 2006, **47**, 123.
16. S. A. Piletsky, K. Karim, E. V. Piletska, C. J. Day, K. W. Freebairn, C. Legge and A. P. F. Turner *Analyst,* 2001, **126**, 1826.
17. S. Subrahmanyam and S. Piletsky, *Combinatorial Methods for Chemical and Biological Sensors*, eds. R. A. Potyrailo and V. M. Mirsky, Springer, 2009, p.135.
18. E. Piletska, S. S. Piletsky, A. Guerreiro, K. Karim, M. Whitcombe and S. A. Piletsky, *J. Chin. Adv. Mater. Soc*., 2014, **2**, 118.
19. S. Subrahmanyam, A. Guerreiro, A. Poma, E. Moczko, E. Piletska and S. Piletsky, *Eur. Polym. J*., 2013, **49**, 100.
20. E. V. Piletska, A. R. Guerreiro, M. Romero-Guerra, I. Chianella, A. P. F. Turner and S. A. Piletsky, *Anal. Chim. Acta*, 2008, **607**, 54.

**For Table of Contents Use Only**

# Magnetic high throughput screening system for the development of nano-sized molecularly imprinted polymers for controlled delivery of curcumin

Elena V. Piletska,* Bashar Abd Hatem, Agata S. Krakowiak, Anitha Parmar, Demi L. Pink, Katie S. Wall, Luke Wharton, Ewa Moczko, Michael J. Whitcombe, Kal Karim, Sergey A. Piletsky

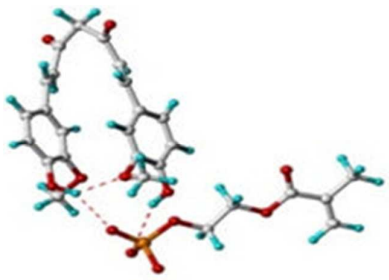

A novel format of the microtitre plate equipped with magnetic inserts allows rapid and cost-effective development of the controlled release materials.